Evolution of the lava flow field by daily thermal and visible airborne surveys

Letizia Spampinato[1,2], Sonia Calvari[1], Andrew J.L. Harris[3], Jonathan Dehn[4]

1 - Istituto Nazionale di Geofisica e Vulcanologia, sezione di Catania, Piazza Roma 2, 95123 Catania, Italy

2 - Department of Geography, University of Cambridge, Cambridge, CB2 3EN, UK

3 - HIGP/SOEST, University of Hawai'i, Honolulu, Hawaii, USA

4 - Alaska Volcano Observatory, Geophysical Institute, University of Alaska Fairbanks, Fairbanks, USA

Abstract

On 28 December 2002, an effusive flank eruption started at Stromboli volcano (Aeolian Islands, Italy). This lasted until 22 July 2003 and produced two lava flow fields that were emplaced onto the steep slopes of Sciara del Fuoco. The first flow field was fed by a vent that opened at 500 m elevation and was active between 30 December 2002 and 15 February 2003. The second was supplied by a vent at 670 m and was emplaced mainly between 15 February and 22 July 2003. Here we review the lava flow field emplacement based on daily thermal and visual surveys. The variable slopes on which the lava flowed yielded an uncommon flow field morphology. This resulted in a lava shield in the proximal area where flow stacking and inflation caused piling up of lava due to the relatively flat ground. The proximal area was characterized by a complex network of tumuli and tube-fed flows associated. The medial-distal lava flow field was emplaced on an extremely steep zone. This area showed persistent flow front crumbling, producing a debris field on which emplaced lava flows formed lava channels with excavated debris levées. This eruption provided an exceptional opportunity to examine the evolution of lava flow fields emplaced on steep slopes, and proved the usefulness of thermal imagers for safe and efficient monitoring of the active lava flows. In addition, thermal monitoring allowed calculation of quantitative parameters, such as effusion rate, allowing constraint of the time varying nature of supply to this eruption.

Keywords: Flank effusive eruption, Lava flow field, Slope gradient, Effusion rate, Thermal imaging

1. Introduction

Although Stromboli volcano is well known for its persistent explosive activity, effusive flank eruptions are also common and have a recurrence time of 5-15 years during the last few centuries (Barberi et al., 1993). Effusive activity does not pose a serious threat to the local community, lava emplacement occur exclusively on the barren Sciara del Fuoco (SDF) depression that cuts the NW flank of the volcano. The two previous effusive flank eruptions occurred in 1975 and 1985-86, descriptions of which are provided by Capaldi et al. (1978) and De Fino et al. (1988), respectively.

The 2002-3 eruption was the first of Stromboli's effusive eruptions for which a large amount of observational and geophysical data were available from continuous monitoring and routine observations. The allowed detailed reconstruction of the chronology of vent opening (Calvari et al., 2005), the processes of lava flow field growth (Lodato et al., 2007), quantification of effusion rate and accumulated lava volume (Calvari et al., 2005; Harris et al., 2005) the volume lost to the sea (Baldi et al., 2008), sliding episodes that occurred at the lava flow field (Falsaperla et al., 2008), and the relationship between effusive flank activity and summit explosive activity (Ripepe et al., 2005).

Volcanological observation has recently been improved by the advent of portable thermal imaging cameras which allow thermal mapping and tracking of active volcanic features (e.g., Calvari and Pinkerton, 2004; Andronico et al., 2005; Burton et al., 2005; Calvari et al., 2005, 2006; Harris et al., 2005; Patrick et al., 2007; Spampinato et al., in press). The use of the thermal camera to record the dynamics of the 5 April 2003 paroxysm at Stromboli is reviewed in Harris et al. (this volume) and detailed in Calvari et al. (2006). However, thermal camera was also used during Stromboli's 2002-3 effusive eruption to monitor the emplacement of the lava flow field and to infer processes of flow field growth, as described in Calvari et al. (2005), Harris et al. (2005) and Lodato et al. (2007). In addition, Ripepe et al. (2005) used satellite-based (MODIS-derived) volume flux data to show how the decline in effusion rate recorded during the eruption related to the re-establishment of "normal" Strombolian activity at the system. We here provide a review of the complex processes that occurred during this effusive eruption, the unusual emplacement mechanisms observed for these lava flows erupted onto steep slopes, and the time varying character of the effusion rates.

2. Methodology

During the 2002-3 effusive eruption daily monitoring performed using a hand-held infrared thermal camera (Forward Looking InfraRed, FLIR Systems), as well as satellite (AVHRR and MODIS) images and digital cameras proved essential for the tracking of lava flow field development and for the retrieval of daily variations in apparent temperature and effusion rate. Analysis of thermal images allowed daily mapping of active lava flows and the identification of lava flow field features, such as

lava channels, lava tubes, ephemeral vents, skylights, and tumuli. Precise feature location and dimension estimates were obtained using laser ranger finders as well as triangulation using FLIR and digital camera images, with thermal and visible images being geo-located using GPS and ground control points. The quantitative analysis of thermal images proved useful to estimate temperatures of specific targets, thermal fluxes, and thus daily effusion rates. For this purpose, daily helicopter flights were performed at an altitude of ~1 km, each day repeating the same flight path to gather comparable thermal data of the entire lava flow field, as well as of the summit craters. Simultaneously, measurements of points, fixed using hand-held GPS, were carried out for pathlength estimation necessary for applying atmospheric corrections and for pixel size calculations. These methodologies are detailed in Calvari et al. (2005), Harris et al. (2005), and Lodato et al. (2007).

3. Chronology of the eruption

After several months of strong explosive activity at the summit craters (Calvari et al., 2005; Burton et al. this volume), on 28 December the first lava flow was erupted from a 300 m long, NE-SW trending fissure that opened at the northeastern flank of Crater 1 (CR1 or North East Crater, NEC) (Fig. 1). This extended from the ~750 m elevation down to ~600 m (Calvari et al., 2005; Lodato et al., 2007), draining the shallow system immediately below the summit craters (Calvari et al., 2005). Debris from the breached flank of the crater mixed with a fast-moving lava flow and formed a hot avalanche that flowed down the SDF, reaching the sea at Spiaggia dei Gabbiani (Fig. 1) and producing a ~4 m thick reddish deposit of subrounded lava clasts and fine-grained ashy matrix (Calvari et al., 2005; Pioli et al. this volume). This deposit was covered almost immediately by two 'a'a lava flows fed by the lowest segment of the eruptive fissure. These lava flows entered the sea after only 10-20 minutes after the eruption began, to give a time averaged velocity of 4-9 km h^{-1} (Lodato et al., 2007). The flows showed evidence of sliding, so that this velocity may well have been enhanced by the flows sliding down the steep slopes of the SDF (Lodato et al., 2007). The western flow reached the sea at Spiaggia dei Gabbiani building a ~70 m wide and 2 m thick lava delta (Calvari et al., 2005; Lodato et al., 2007). After two hours of hiatus, the distal end of the eruptive fissure fed a new flow that was emplaced towards the middle section of of the SDF.

Figure 1

By the morning of 29 December at 11:30 local time (all times are local) lava flows of the previous day were already inactive. Effusive activity resumed late in the same day. On the morning of the 30th, a thermal survey revealed the inactive 28 and 29 December flows, the cooling 30 December flows,

and the opening of an effusive vent in the eastern upper portion of SDF at the 670 m elevation (Fig. 1). It also revealed the development of a high-temperature fracture system along the SDF (Calvari et al., 2005). Within a few hours, widening and extension of these fractures triggered the failure of two large portions of SDF (5 x 10^5 and 6 x 10^6 m^3 respectively), which led to the generation of tsunami waves as they entered the sea (Bonaccorso et al., 2003). This loss in mass, along with the development and deepening of the fractures, allowed passive magma intrusion (Bonaccorso et al., 2003; Calvari et al., 2005) and eruption of lava through two new effusive vents at 500 and 550 m elevation, respectively (Fig. 1). While the 550 m vent was active only for a few days, the 500 and 670 m vents were active for longer periods and built two spatially and temporally separated lava flow fields (Fig. 1). Whereas the 500 m elevation vent fed lava flows until its abrupt closure on 15 February 2003, the 670 m vent was sporadicly active during the first month and a half of eruption, and stabilized in coincidence with the shutting of the lower 500 m vent.

Figure 2

Calvari et al. (2005) attributed the migration of effusive vents to higher elevations, with activity shifting from the 500 m to the 670 m vent on 15 February, to changes in magma level within the upper conduit (Fig. 2). According to these authors, this process was enhanced by the proximity of the central upper conduit to the topographic surface due to the loss in rock volume after the 30 December landslides.

The 500 and 550 m vents erupted lava flows that filled the central-western sector of the SDF and entered the sea forming lava deltas (lava field in dark grey in Fig. 1). The 670 m vent also produced lava flows that reached the sea (lava field in light grey in Fig. 1). However, after the occurrence of a major explosive event on 5 April, lava flows remained mainly confined to the proximal area until the end of the effusive eruption between 21 and 22 July 2003. A decline in lava output during the final months of the eruption was concomitant with the restart of the strombolian activity at the summit craters (Ripepe et al., 2005). This suggested the gradual return of the volcanic system to the steady pre-eruptive state (Calvari et al., 2005; Ripepe et al., 2005; Salerno et al., 2006).

4. Lava flow field emplacement mechanisms

The first lava flows of 28 and 29 December were erupted from the lower segment of the eruptive fissure with high effusion rates, the eruption rate on 28 December being ~280 m^3 s^{-1}. Such high effusion rates are to be expected in a situation where rapid drainage of a volcanic conduit occurs (e.g., Bertagnini et al., 1990; Tazieff, 1977). In the proximal area, these flows had an 'a'a surface

morphology with narrow lava channels. Distally they formed thick aprons of lava mixed with debris (Calvari et al., 2005). Features of the flows in section, as exposed at the Spiaggia dei Gabbiani beach (i.e., high amounts of entrainment, lack of basal clinker, patterns of shear, and incorporation of underlying material), are consistent with the flows sliding down the steep underlying slope which was composed unconsolidated material capable of easy entrainment (Lodato et al., 2007). After this first stage of effusion, in which lava was supplied directly from a fissure opening from the base of the summit craters, the 7-month-long flank eruption was fed by the opening of topographically lower effusive vents. Here we detail the emplacement, development, closure, and features of the individual lava flow fields produced by the main effusive vents that opened at the 500 and 670 m elevations respectively.

4.1. Lava flow field fed by the 500 m vent: 30 December 2002-15 February 2003

Between 30 December 2002 and 15 February 2003, persistent activity from the 500 m vent built an 'a'a compound lava flow field that was emplaced in the middle of SDF within the largest of the two 30 December landslide scars (Bonaccorso et al., 2003; Calvari et al., 2005) (Figs. 1 and 3). This sector of the SDF was affected by collapses from failures at the boundaries of the landslide scars, as well as grain flow from failure at the active lava flow fronts (Lodato et al., 2007). Accumulation of this mixed debris modified locally the topography, influencing lava flow paths and the morphology of lava flow channels. In fact, the combination of high slope gradient (~35-45°) and the loose debris accumulation, promoted the lava flow to mechanically erode the undelying debris, thus developing lava flow channels with excavated levées (Calvari et al., 2005 in Fig. 3, I).

Figure 3

Lava flowed as single units (Fig. 3, IIb), branched flows (Fig. 3, IIc), and within lava tubes, which fed flow from ephemeral vents and/or skylights (Fig. 3, IId) (Calvari et al., 2005).

The development of lava tubes on these steep slopes was favoured by the continuous supply of debris from the landslide scar which buried segments of active lava flows. The debris carpet would cover the active lava flows, which emerged from beneath the carpet at topographic breaks-in-slope. This initially gave the impression of effusive vent migration and down slope propagation of the feeder dike (Calvari et al., 2005).

The steady overlapping of lava flows formed a triangular lava flow field that eventually filled the largest of the 30 December landslide scars (Calvari et al., 2005). This implied that, in 19 days of activity, the 500 m elevation vent erupted a minimum lava volume ~6 x 10^6 m^3 (i.e., the volume of

the filled scar), to give a time-averaged discharge rate of ~3.7 m^3 s^{-1} (Calvari et al., 2005; Lodato et al., 2007). Assuming a vesicularity of ~22 ± 12% (Harris et al., 2000), this yielded a dense rock equivalent (DRE) discharge rate of 2.9 ± 0.4 m^3 s^{-1} (Calvari et al., 2005).

4.2. Lava flow field fed by the 670 m vent: 15 February - 22 July 2003

On 15 February, the 500 m elevation vent ceased its activity and effusion shifted to the bench at the base of CR1, where effusion had occurred sporadically between the end of December 2002 and February 2003 (Calvari et al., 2005; Lodato et al., 2007). Over the time, on this relatively gentle topography, lava flows fed by the 670 m vent built a complex, compound lava flow field (Fig. 1), within which a number of secondary opened to feed tube-fed lava flows that piled up around the vent. The combination of lava flow stacking and inflation resulted in construction of a ~50 m thick lava shield around the vent (Calvari et al., 2005; Lodato et al., 2007) (Fig. 4). The development of lava tubes that were efficient in transferring lava from the main vent (670 m elevation) to lower elevations, also resulted in lava flow field extension. This style of lava emplacement characterized the whole effusive period. Activity from this vent persisted through the 5 April explosive event, which changed the flow field morphology and SDF topography due to the accumulation of the 5 April deposits (Calvari et al., 2005; Lodato et al., 2007). Thus we split the development of the 670 m lava flow field into two periods spanning 15 February until 5 April, and 5 April until the eruption end on 22 July.

4.2.1. Lava flow field development before the 5 April paroxysm

Effusive activity fed by the 670 m vent before 15 February produced numerous lava flows that spread westwards but remained confined in the flat proximal area, forming a compound flow field. Flow which extended northwards moved onto the steep slopes of the SDF excavating narrow lava channels and feeding crumbling flow fronts (Lodato et al., 2007). As a result of flow front crumbling, much of the volume of these flows tumbled into the sea. Beginning on 15 February, lava rarely flowed down SDF and remained laregly confined to the bench between 670 and 560 m (Fig. 4a). Here the continuous piling up of sheet-flow lava units erupted by the 670 m vent led to the development of a dome-like feature within the vent region. This structure was the result of endogenous growth due to lava injection and sheet flow inflation, as well as the exogenous piling up of flow units at the surface (Lodato et al., 2007). Following the classification of Walker (1991), Rossi and Gudmundsson (1996) and Duncan et al. (2004), we term this feature a tumulus. This tumulus (Tumulus A, TA) was the first in a series of four tumuli (Tumulus B, TB; Tumulus C, TC; and Tumulus D, TD in Fig. 4 and Tab. 1) that formed across the proximal area. Except for TA,

207 which was the main tumulus [Primary focal tumulus following Duncan et al. (2004)] and developed
208 over the main effusive vent, the others formed at exits of lava tubes which opened at topographic
209 breaks-in-slope (Fig. 4).
210 **Figure 4**
211
212 TA fed lava flows from its base and, eventually, from its summit until 16 February, when the
213 development of a lava tube from its foot along the NE trending fissure transferred lava output to a
214 location 20-30 m below the tumulus (Fig. 4). This tube became the main arterial path through which
215 lava could reach the surface (Lodato et al., 2007). Successively, a number of short-lived lava flows
216 piled up at the exit of this tube, generating a second focal tumulus structure (Tumulus B, TB). By 17
217 March, the continuous repetition of this process had produced the development of additional tubes
218 and tumuli (Tumulus C and Tumulus D, TC and TD respectively), resulting in a complex network of
219 tumuli connected by lava tubes (Fig. 4).
220
221 *4.2.2. Lava flow field development after the 5 April paroxysm*
222 The 5 April paroxysm covered the proximal lava shield with a ~10 m thick carpet of pyroclastics
223 (Calvari et al., 2005; 2006; Lodato et al., 2007) (Figs. 5a and b). This caused a significant
224 morphological change in the flow field surface, filling the depressions between single lava flows,
225 and in the topography of SDF, extending the proximal bench ~10 m down slope (Fig. 5). However,
226 the paroxysm did not affect lava effusion or the tube-tumulus network. In fact, after less than two
227 hours, lava emerged along the new break-in-slope, flowing through three main vents (Calvari et al.,
228 2005; Lodato et al., 2007) (Figs. 5a and b). Each of these vents was directly linked to the three
229 buried tumuli (TB, TC and TD) through tubes excavated within the low density and poorly
230 consolidated debris (Fig. 5b).
231
232 **Figure 5**
233
234 By 7 April, three second-order tumuli (Tumulus 1, T1; Tumulus 2, T2; and Tumulus 3, T3; in
235 Fig. 6d) had developed at the location of the three vents (Fig. 5b, Tab. 1). These linked effusion back
236 to the three parental tumuli (TB, TD and TC), as shown in Fig. 5d. By 11 April, both T2 and T3 had
237 deactivated, marking the death of both TD and TC and the beginning of the waning phase of the
238 effusive activity (Lodato et al., 2007). From this point onwards, lava output focused at T1, thus
239 along the TA-TB-T1 alignment (Fig. 6a).

The concentration of lava output at T1 allowed lava flows to extend down to the 300 m elevation, and triggered the renewal of activity in the proximal area. Here, TB emerged gradually from the 5 April pyroclastic deposit, displaying degassing and spattering activity that, by 18 April, had produced a hornito (Fig. 6b). TB fed short, channelized lava flows which were emplaced onto its flanks, thus promoting further exogenous growth of TB. By 2 May, a second hornito had developed.

Figure 6

Effusion at T1 remained steady until the first half of June, when activity migrated back up the lava tube linking T1 with TB, over which four additional tumuli formed (T1.1, T1.2, T1.3, and T1.4, Fig. 6b). We named these third-order tumuli "ephemeral tumuli" (Fig. 6b, Tab. 1). Each formed progressively up-tube and were built by the superposition of short lava flows fed by skylights (Fig. 6b). This mechanism of lava flow field regression persisted until late July, after which effusion occurred only at TB. On 22 July the effusive eruption ended.

5. Main parameters controlling lava flow emplacement

5.1. Effusion Rate

We present here data from Harris et al. (2005), Calvari et al. (2005) and Lodato et al. (2007), which combine effusion rates obtained from 64 FLIR thermal images and 25 Advanced Very High Resolution Radiometer (AVHRR) images (Fig. 7). As shown by Calvari et al. (2005) and Harris et al. (2005), thermally-derived effusion rates from both data sets are consistent with field-based effusion rate measurements, with near-simultanoeus results obtained from the FLIR and AVHRR data sets being consistent with one another.

Figure 7

Following the initial peak at the onset of the effusive activity on 28 December, effusion rate was characterized by a gradually declining trend (black-dashed line in Fig. 7) from 0.6-0.7 $m^3 s^{-1}$ in January to 0.1 $m^3 s^{-1}$ by July (Calvari et al., 2005; Lodato et al., 2007). However, this behavior was not linear and displayed some significant fluctuations which allowed us to split the effusive eruption into four main periods (1, 2, 3 and 4 in Fig. 7).

The first period (1) corresponded to the emplacement of the 500 m-fed lava field. This showed relatively high effusion rates (0.6-0.5 $m^3 s^{-1}$) that in the middle of January began to decline. By 13 February, two days before the shut down of the 500 m vent, effusion decayed to 0.3 $m^3 s^{-1}$. The

second period (2) displayed a phase of moderate effusion rate (0.5 m^3 s^{-1}) with a peak around 4 March. By 24 March, effusion decreased again reaching ~0.1 m^3 s^{-1}. The remaining days of this period were characterized by pulses, with two main peaks around 10 April and 5 May, separated by a smaller peak between 22 and 28 April (Fig. 7). During the third period (3) effusion rates were stable and low (~0.1 m^3 s^{-1}). The fourth period (4) began around 26-27 May with an abrupt increase in effusion rate that peaked at 1.1 m^3 s^{-1} on 3 June. After that, effusion rates gradually declined to ~0.1 m^3 s^{-1} by 3 July remaining low until the end of the eruption on 22 July (Fig. 7).

5.2. Sciara del Fuoco topography

It is well known that topography can control lava flow paths and lava flow field morphology (e.g., Walker, 1973, 1991; Kilburn & Lopes, 1991; Calvari and Pinkerton, 1998). To check the control of slope on flow field morphology, Lodato et al. (2007) divided the SDF into four sectors: a proximal, low gradient zone, an intermediate gradient, medial zone, a high-gradient, medial-distal zone, and a low-gradient, distal-toe zone and examined the morphologies of each.

Figure 8

1. Low gradient proximal zone

This zone represents the bench at the base of CR1 and proximal area of the lava field (Fig. 8a). Here the gentle slopes, varying between 0 and 15°, allowed both endogenous (inflation and tumuli) and exogenous (lava piling up) processes. Tumuli, tumuli-fed ephemeral vents, 'a'a lava flows, tubes, skylights, and tube-fed flows built a complex flow field. Piling up of these features resulted in the formation of a proximal lava shield. Additionally, although the activity was dominated by emplacement of 'a'a lava flows, this was the only zone where pahoehoe flows were emplaced.

2. Intermediate gradient medial zone

This zone includes the lava flow field emplaced between the 600 and 580 m elevations, where slopes were 15 to 30° (Fig. 8a). It represents a transitional region between the low gradient proximal zone and the steeper distal zone. Here lava formed 'a'a lava flows, channels, tubes, tube-fed ephemeral vents, with channels being characterized by excavated levées (Calvari et al., 2005).

3. High gradient medial-distal zone

This zone was located below the 580 m elevation and was characterized by slopes greater than 30° (Fig. 8b). Here 'a'a lava flows showed channels with excavated levées, lava tubes where segments of active lava flows were buried by debris, tube-fed ephemeral vents, skylights, and skylight-fed flows. Furthermore, due to the high gradient of the slope, this zone was the site of continuous lava flow front collapses.

309 *4. Low gradient distal-toe zone*

310 This last zone comprises two low gradient areas. The first is located on the eastern edge of SDF, and
311 extends from the 300 m elevation to sea level (Spiaggia dei Gabbiani) (Fig. 8c). The second is
312 located 500 m West from the eastern edge of the SDF, and extends from the 30 m elevation to the
313 sea. Both zones were characterized by slopes varying between 5 and 15° promoting 'a'a flow,
314 classical lava channels, dispersed flows, sea-entry flows, and lava deltas (Fig. 8c).

315

316 **6. Discussion**

317 The 2002-3 effusive flank eruption of Stromboli provided a unique opportunity to study lava flow
318 field morphology and emplacement on steep slopes. From a proximal shield, lava flowed through
319 lava channels and tubes, to feed the medial-distal portion of the flow field. Here the flows were
320 emplaced on extremely steep slopes that promoted sliding, front crumbling, and autobrecciation.
321 This caused an effective removal of lava volume from the slope to the sea, and significantly reduced
322 the measurable final volume of the flow field. In June 2004, for instance, the remaining volume of
323 lava on the SDF was ~2 x 10^6 m^3. Based on the discrepancy between the time-integrated eruption
324 rate measurements and the final flow field volume, 70% of the erupted volume is missing (Calvari et
325 al., 2005). Lava front crumbling together with landslides, from the 30 December landslide scar, was
326 responsible for the formation of a distal talus and burial of active flows to enhance tube formation. In
327 the medial-distal zones, accumulation of the fine-grained portion of this debris allowed for the
328 formation of narrow lava channels characterized by excavated levées when active flow overrode
329 such debris.

330 The morphology of the lava flows was not only governed by the slope gradient, but also by
331 effusion rate. During peaks in effusion rate, single 'a'a lava flows entered the sea, causing explosions
332 at the flow fronts and accumulation of aprons of debris at the foot of the SDF (Fig. 3, IIa,b).
333 Decreases in effusion rate resulted in flow branching (Fig. 3, IIc) to feed flow fields that widened the
334 lava field in the middle of the SDF. Further decreases in effusion rate caused lava tube growth and
335 tube-and-skylight-fed lava surface flows (Fig. 3, IId). Commonly, in the proximal area, decreases in
336 effusion rate corresponded to the growth of many small, short-lived vents. This suggested that high
337 numbers of vents did not necessary imply high effusion rates, but instead the incapability of the
338 supply system to feed single, well-fed and long-lasting lava flows (Lodato et al., 2007; Spampinato
339 et al., in press). The reverse was true when, after 11 April, effusion became focused at tumulus T1,
340 and flow lengths increased. However, this was not triggered by an increase in the total effusion rate,
341 but by an increase in the local effusion rate to the T1-fed flows due to the concentration of the entire
342 flux at one tumulus instead of three.

Overall, effusion rate revealed a gradual decreasing trend during the eruption (Fig. 7). This declining rate has been shown to correlate with an increase in the free-surface level in the central conduit and the number of strombolian events recorded at the crater terrace (Ripepe et al., 2005). Ripepe et al. (2005) concluded that reduced tapping of the central column by the flank effusive activity allowed magma levels in the conduit, and normal explosive activity, to steadily recover (Ripepe et al., 2005). However, this trend of declining effusion was interrupted by three significant peaks, each linked to distinct eruptive events, these being the sudden onset of effusive activity on 28 December, the 5 April paroxysm, and an increase in strombolian activity at the summit craters during late May. The latter two revivals in effusion rate were thus associated with increases in the explosive activity at the summit craters and was followed by a period of steady effusion rate decline (Fig. 7). This suggested that the eruption may have been punctuated by the arrival of three major batches of magma, the first causing the onset of the effusive eruption on 28 December, and the second and third causing increases in effusion around the time of increase in explosive activity (Lodato et al., 2007). On a finer time scale, Harris et al. (2005) noted increases in effusion lasting a day or so following increases in vent temperature at the CR1. These were assumed to result from short-term oscillations in the magma level in the central conduit which increased the driving pressure for the magma erupting from the lateral vent, plausible increases in the magma-static head being consistent with the subsequent increase in effusion rate.

Because it was largely removed by collapse, the 2002-3 effusive flank eruption produced a final lava flow field that was hard to distinguish from the pre-existing morphology of the SDF. Mostly this was because it did not exist - apart from the proximal shield it had all crumbled into to Mediterranean. However, a total DRE volume of ~6 x 10^6 m^3 was calculated by Calvari et al. (2005). This, given an emplacement time of 156 days, yields mean output rate of ~0.5 m^3 s^{-1}. This is comparable to the mean output rate of the 1985-86 effusive eruption (0.3±0.2 m^3 s^{-1}, Rossi and Sbrana, 1988; Nappi and Renzulli, 1989, Harris et al., 2000), as well as the time-average supply rate calculated for normal Strombolian activity (0.1-0.6 m^3 s^{-1}, Allard et al, 1994; Harris and Stevenson, 1997). This led Harris et al. (2005) to conclude that "the similarity between the erupted fluxes during these (2002-3 and 1985-6) effusive phases and the time-averaged supply during normal, persistent (non-effusive, Strombolian) activity, leads us to suggest that the 2002-3 eruption comprises bleeding of the conduit at a flux typical for Stromboli. The difference between the non-effusive and effusive phases is that the ascending (supplied) volume is not erupted in the former case, but instead degasses and descends in the convecting conduit.

8. Conclusions

During the 2002-3 effusive eruption of Stromboli, daily thermal surveys using a hand-held FLIR thermal camera allowed monitoring of the lava field emplacement and the retrieval of effusion rates. This 7-month long eruption was characterized by low effusion rates (<1 m^3 s^{-1}), which produced ~6 x 10^6 m^3 of lava and uncommon lava flow field morphologies. These uncommon morphologies were strongly controlled by the steep slopes on which lava emplaced. The result was a number of characteristic lava field features. Several papers deal with basaltic lava morphology flowing on relatively gentle surfaces, our contribution provides a framework for tracking, understanding and interpreting the evolution of lava flow fields emplaced on steep slopes. In addition, the thermal camera-data- and satellite-data- based effusion rates improved our understanding of the time-varying nature of effusion at Stromboli, and its relation to the magma supply to the shallow system.

Acknowledgments

Two anonymous referees are acknowledged for their constructive reviews that significantly improved the manuscript. LS thanks the project ‘Sviluppo di sistemi di monitoraggio’ (Dipartimento di Protezione Civile di Regione Sicilia, INGV Catania Section-Italy) for funding doctoral research.

445 **References**

446 Allard P., J. Carbonelle, N. Métrich, H. Loyer and P. Zettwoog, Sulphur output and magma
447 degassing budget of Stromboli volcano, *Letters to Nature*, 368, 326-330, 1994.

448 Andronico D., S. Branca, S. Calvari, M. Burton, T. Caltabiano, R.A. Corsaro, P. Del Carlo, G. Garfì,
449 L. Lodato, L. Miraglia, F. Murè, M. Neri, E. Pecora, M. Pompilio, G. Salerno and L.
450 Spampinato, A multi-disciplinary study of the 2002-03 Etna eruption: insights into a complex
451 plumbing system, *Bull. Volcanol.*, 67, 314-330, 2005.

452 Baldi P., M. Coltelli, M. Fabris, M. Marsella and P. Tommasi, High precision photogrammetry for
453 monitorino the evolution of the NW flank of Stromboli volcano during and after the 2002-2003
454 eruption, Bull. *Volcanol.*, 70, 703-715, 2008.

455 Barberi F., M. Rosi and A. Sodi, Volcanic hazard assessment at Stromboli based on review of
456 historical data, *Acta Vulcanologica*, 3, 173-187, 1993.

457 Bertagnini, A., S. Calvari, M. Coltelli, P. Landi, M. Pompilio and V. Scrivano, The 1989 eruptive
458 sequenze, in "*Mt. Etna: the 1989 eruption", Barberi F., Bertagnini A., Landi P. eds, CNR GNV*
459 *Special Issue, Giardini, Pisa*, 10-22, 1990 .

460 Bonaccorso, A., S. Calvari, G. Garfi, L. Lodato and D. Patane, Dynamics of the December 2002
461 flank failure and tsunami at Stromboli volcano inferred by volcanological and geophysical
462 observations, *Geophys. Res. Lett.*, 30(18), 1941, doi:10.1029/2003GL017702, 2003.

463 Burton M., S. Calvari, L. Spampinato, L. Lodato, N.A. Pino, E. Marchetti and F. Murè, Volcanic and
464 seismic activity at Stromboli preceding the 2002-03 eruption. *This volume*.

465 Burton M.R., M. Neri, D. Andronico, S. Branca, T. Caltabiano, S. Calvari, R.A. Corsaro, P. Del
466 Carlo, G. Lanzafame, L. Lodato, L. Miraglia, G. Salerno and L. Spampinato, Etna 2004-2005:
467 An archetype for geodynamically-controlled effusive eruptions, *Geophys. Res. Lett.*, 32, L09303,
468 doi:10.1029/2005GL022527, 2005.

469 Calvari, S. and H. Pinkerton, Formation of lava tubes and extensive flow field during the 1991-93
470 eruption of Mount Etna, *J. Geophys. Res.*, 103, 27,291-27,303, 1998.

471 Calvari S. and H. Pinkerton, Birth, growth and morphologic evolution of the 'Laghetto' cinder cone
472 during the 2001 Etna eruption, *J. Volcanol. Geotherm. Res.*, 132, 225-239, 2004.

473 Calvari, S., L. Spampinato, L. Lodato, A.J.L. Harris, M.R. Patrick, J. Dehn, M.R. Burton and D.
474 Andronico, Chronology and complex volcanic processes during the 2002-2003 flank eruption at
475 Stromboli volcano (Italy) reconstructed from direct observations and surveys with a hand-held
476 thermal camera, *J. Geophys. Res.*, 110, B02201, doi:10.1029/2004JB003129, 2005.

Calvari, S., L. Spampinato and L. Lodato, The 5 April 2003 vulcanian paroxysmal explosion at Stromboli volcano (Italy) from field observations and thermal data, *J. Volcanol. Geotherm. Res.*, 149 (1-2), 160-175, 2006.

Capaldi G., I. Guerra, A. Lo Bascio, G. Luongo, R. Pece, A. Rampolla, R. Scarpa, E. Del Pezzo, M. Martini, M.R. Ghiara, L. Lirer, R. Munno and L. La Volpe, Stromboli and its 1975 Eruption, *Bull. Volcanol.*, 41 (3), 259-285, 1978.

De Fino, M., L. La Volpe, S. Falsaperla, G. Frazzetta, G. Neri, L. Francalanci, M. Rosi and A. Sbrana, The Stromboli eruption of December 6, 1985 - April 25, 1986: volcanological, petrological and seismological data, *Rend. Soc. It. Min. Petr.*, 43, 1021-1038, 1988.

Duncan, A.M., J.E. Guest, E.R. Stofan, S.W. Anderson, H. Pinkerton and S. Calvari, Development of tumuli in the medial portion of the 1983 'a'a flow-field, Mount Etna, Sicily, *J. Volcanol. Geotherm. Res.*, doi:10.1016/S0377-0273(03) 00344-5, 2004.

Falsaperla S., V. Maiolino and S. Spampinato, Sliding episodes during the 2002-2003 Stromboli lava effusion: Insights from seismic, volcanic, and statistical data analysis, *Geochemistry, Geophysics, Geosystems (G-3)*, 9 (4), Q04022, doi:10.1029/2007GC001859, ISSN: 1525-2027, 2008.

Harris A.J.L. and D.S. Stevenson, Thermal observations of degassing open conduit and fumaroles at Stromboli and Vulcano using remotely sensed data. *J. Volcanol. Geotherm. Res.*, 76, 175-198, 1997.

Harris, A.J.L., J.B. Murray, S.E. Aries, M.A. Davies, L.P. Flynn, M.J. Wooster, R. Wright and D.A. Rothery, Effusion rate trends at Etna and Krafla and their implications for eruptive mechanisms, *J. Volcanol. Geotherm. Res.*, 102, 237-270, 2000.

Harris, A., J. Dehn, M. Patrick, S. Calvari, M. Ripepe and L. Lodato, Lava effusion rates from hand-held thermal infrared imagery: An example from the June 2003 effusive activity at Stromboli, *Bull. Volcanol.*, 68, 2, 107-117, 2005.

Harris A.J.L., M. Ripepe, S. Calvari, L. Lodato and L. Spampinato, The 5 April 2003 explosion of Stromboli: Timing of eruption dynamics using thermal data. *This volume*.

Kilburn C. and R. Lopes, General Patterns of Flow Field Growth: Aa and blocky lavas. *J. Geophys. Res.*, 96 (B12), 19721-19732, 1991.

Lodato, L., L. Spampinato, A. Harris, S. Calvari, J. Dehn and M. Patrick, The Morphology and Evolution of the Stromboli 2002-03 Lava Flow Field: An Example of Basaltic Flow Field Emplaced on a Steep Slope. *Bull. Volcanol.*, 69, 661-679, doi: 10.1007/s00445-006-0101-6, 2007.

Nappi G. and A. Renzulli, Stromboli. *Bull Volcanic Eruptions*, 26, 1-3, 1989.

Patrick M.R., A.J.L. Harris, M. Ripepe, J. Dehn, D.A. Rothery and S. Calvari, Strombolian explosive styles and source conditions: insights from thermal (FLIR) video, *Bull. Volcanol.*, 69, 769-784, 2007.

Pioli L., M. Rosi, S. Calvari, L. Spampinato, A. Renzulli and A. Di Roberto, The eruptive activity of 28 and 29 December 2002. *This volume*.

Ripepe M., E. Marchetti, G. Ulivieri, A. Harris, J. Dehn, M. Burton, T. Caltabiano and G. Salerno, Effusive to explosive transition during the 2003 eruption of Stromboli volcano. *Geology*, 33, 341-344, 2005.

Rossi, M. and A. Sbrana, Stromboli. *Bull. Volcanic Eruptions*, 25, 7-8, 1988.

Rossi, M.J. and A. Gudmundsson, The morphology and formation of flow-lobe tumuli on Icelandic shield volcanoes, *J. Volcanol. Geotherm. Res.*, 72, 291-308, 1996.

Salerno G., L. Spampinato, M. Burton, S. Calvari, L. Lodato, T. Caltabiano, D. Andronico, D. Condarelli, V. Longo and F. Muré, Hiatus in the typical strombolian activity during the 2002-03 Stromboli effusive eruption: SO_2 flux degassing and thermal release relationship as a marker of anomalous activity. *GPL Walker Symposium 2006, Reykholt, Reykjavik, Iceland*, 2006.

Spampinato L., S. Calvari, C. Oppenheimer and L. Lodato, Shallow magma transport for the 2002-3 Mt. Etna eruption inferred from thermal infrared surveys, *J. Volcanol. Geotherm. Res., in press*.

Tazieff H., An exceptional eruption: Mt. Nyragongo, Jan. 10^{th} , 1977. *Bull. Volcanol.*, 40, 189-200, 1977.

Walker, G.P.L., Lenghts of lava flows, *Phil. Trans. R. Soc. Lon. A.*, 274, 107-118, 1973.

Walker, G.P.L., Structure, and origin by injection of lava under surface crust of tumuli, “lava rises”, “lava-rise pits”, and “lava-inflation clefts” in Hawaii, *Bull. Volcanol.*, 53, 546-558, 1991.

Table 1. Dates and elevations of tumuli between 15 February and 22 July 2003

Order	Tumulus	Elevation a.s.l. (m)	Classification	Starting day	Last day	Duration (days)
1	TA	670	primary focal	15 February	22 July	156
1	TB	630	secondary focal	18 February	22 July	154
1	TC	600	primary satellite	22 February	11 April	48
1	TD	580	primary satellite	17 March	9 April	23
2	T1	560	secondary satellite	7 April	16 June	70
2	T2	560	secondary satellite	7 April	9 April	2
2	T3	560	secondary satellite	7 April	11 April	4
3	T1.1	560 – 630	ephemeral	25 June	9 July	14
3	T1.2	560 – 630	ephemeral	29 June	5 July	6
3	T1.3	560 – 630	ephemeral	2 July	4 July	2

571 **Figure captions**

572

573 **Figure 1.** Shaded relief map of Stromboli Island showing Sciara del Fuoco, the flank affected by the
574 effusive activity and by the 30 December landslides, the two main summit craters (Crater 1, CR1 and
575 Crater 3, CR3), the NE-trending eruptive fissure in white, the two main effusive vents (500 m vent
576 and 670 m vent), the two distinct lava flow fields (in dark grey the one fed by the 500 m vent and
577 light grey that fed by the 670 m vent), the Spiaggia dei Gabbiani beach, and the landslide scar (gray
578 line) (modified after Calvari et al., 2005).

579

580 **Figure 2.** Qualitative models of Stromboli's 2002-3 effusive eruption showing Sciara del Fuoco
581 (SDF), the site of lava emplacement, and the migration of effusive vent elevations between 28
582 December 2002 and 22 July 2003 (modified after Calvari et al., 2005). In A, three main effusive
583 vents are simultaneously active at 670, 550, and 500 m elevation respectively; in B, only two main
584 vents (670 and 500 m elevation respectively) are feeding lava flows; in C, only the 670 m elevation
585 main effusive vent is active and supplying lava to the three secondary vents below through lava
586 tubes.

587

588 **Figure 3.** I. Cartoon showing the formation of the excavated debris levées along the Sciara del
589 Fuoco. A and B are cross sections through the talus produced by the 30 December landslide events;
590 C and D are their longitudinal sections respectively (modified after Calvari et al., 2005). II. (a) Photo
591 of Sciara del Fuoco with the emplacement of lava flows from the 500 m vent. The white dot
592 indicates the position of the 500 m effusive vent feeding the lava flows shown in (b, c, and d). The
593 white rectangle shows the area of Sciara del Fuoco imaged in b, c, and d. The three thermal images
594 show three different styles of lava flow emplacement associated with effusion rate variations: (b)
595 emplacement of a single lava unit entering the sea with high effusion rates; (c) lava flow branching
596 feeding multiple entries with moderate effusion rates, and (d) development of lava tubes and opening
597 of ephemeral vents with low effusion rates (modified after Calvari et al., 2005).

598

599 **Figure 4.** Photo of the upper portion of the lava flow field (top area of the light-grey lava flow field
600 in Fig. 1) taken on 18 March 2003 during a helicopter survey. The four first-order tumuli (TA, TB,
601 TC and TD) are shown. The white dashed arrows indicate lava tube paths and lava flow direction;
602 the break-in-slope at the ~560 m elevation is also shown (modified after Lodato et al., 2007).

603

Figure 5. (a) photo revealing the condition of the lava shield (the upper portion of the lava flow field in light grey in Fig. 1) covered by the 10 m-thick pyroclastic deposit (area surrounded by the black-dotted line) produced by the 5 April paroxysm and the new break-in-slope shifted ~10 m down slope. (b) is a sketch of the lava shield with its tumuli and lava tubes buried by 5 April deposits, and the new effusive vents that opened along the new break-in-slope ~2 hours after the paroxysm (modified after Lodato et al., 2007). The scale in (b) indicates the maximum width of the lava flow fed by the 670 m vent, measured in April 2003.

Figure 6. (a) Longitudinal section of the lava shield showing the 5 April deposit, two of the first-order of tumuli TA and TB, the second-order tumulus T1, and the lava tube connecting TB to T1. (b) Longitudinal section of the lava shield displaying the 5 April deposit the first hornito that grew up top TB, the lava tube TB-T1, and the third-order tumuli (ephemeral tumuli, T1.1, T1.2, and T1.3) that developed over TB-T1 tube (modified after Lodato et al., 2007).

Figure 7. Seven-point-running mean for effusion rate calculated using the FLIR and AVHRR data. The grey portion of the graph refers to the first effusive period (28 December 2002-15 February 2003) and the white to the second (15 February-22 July 2003). The arrows mark the main events that occurred during the effusive activity, whereas the black-dashed line shows the steady declining trend (modified after Lodato et al., 2007).

Figure 8. Photo showing the eastern edge of Sciara del Fuoco with the four gradient zones. **a**, **b** and **c** are zooms of the gradient areas marked in the main photo: **a** shows the low gradient proximal and the intermediate medial zones (view of the lava shield); **b** the high gradient medial-distal zone; and **c** one of the two low gradient distal-toe zones.

Figures

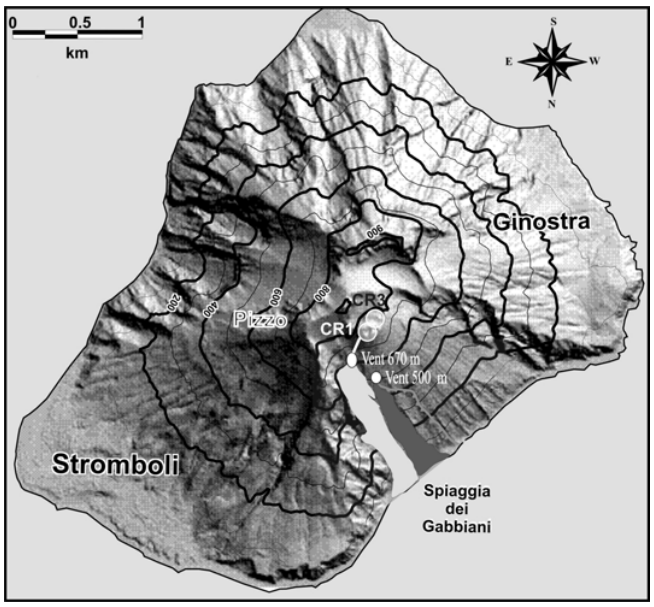

Figure 1

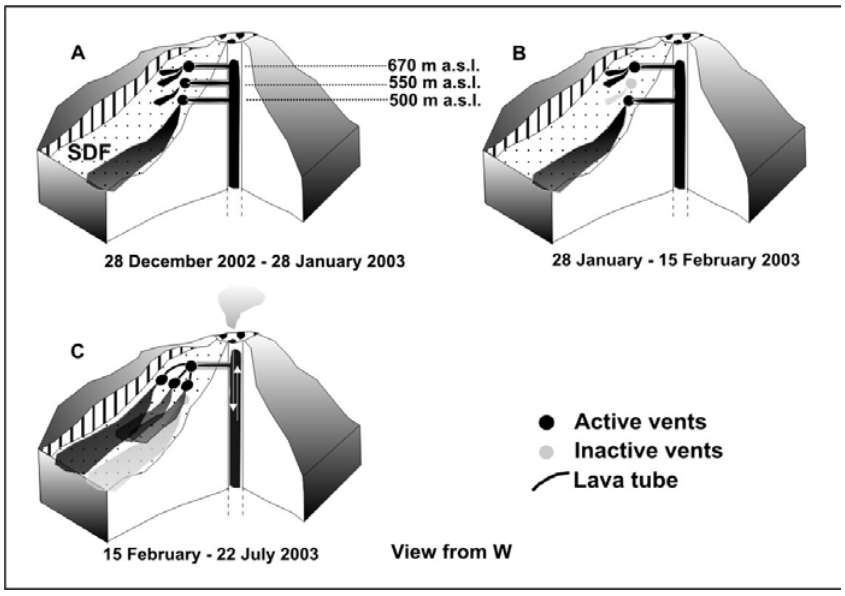
A
670 m a.s.l.
550 m a.s.l.
500 m a.s.l.
SDF
B
28 December 2002 - 28 January 2003
28 January - 15 February 2003
C
Active vents
Inactive vents
Lava tube
15 February - 22 July 2003
View from W

Figure 2

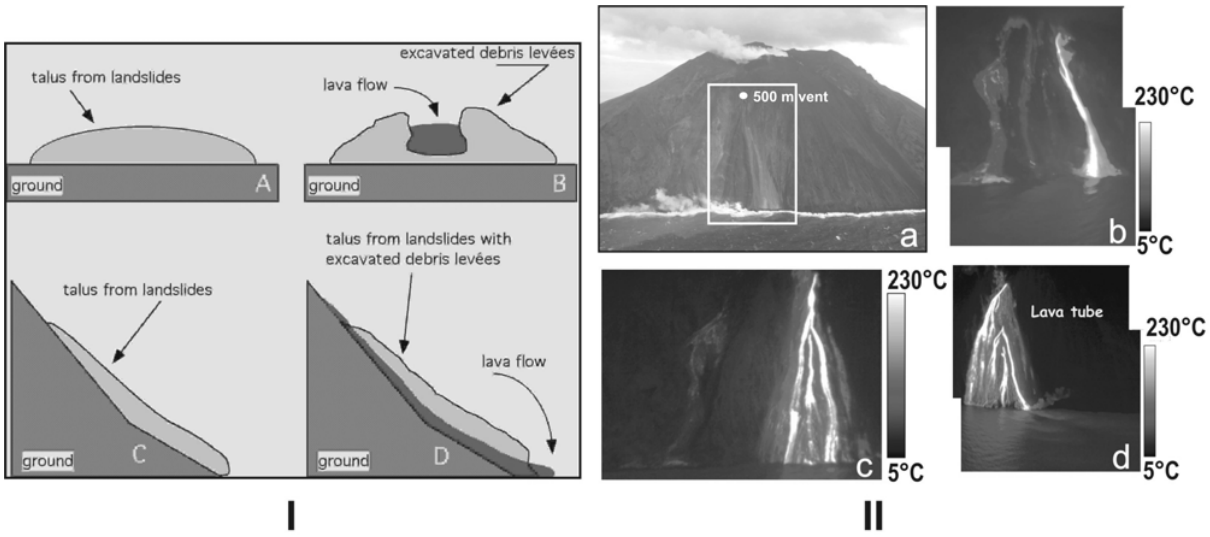
talus from landslides
excavated debris levées
lava flow
ground
A
ground
B
talus from landslides
talus from landslides with
excavated debris levées
lava flow
ground
C
ground
D
I
500 m vent
a
230°C
5°C
b
230°C
5°C
c
Lava tube
230°C
5°C
d
II

Figure 3

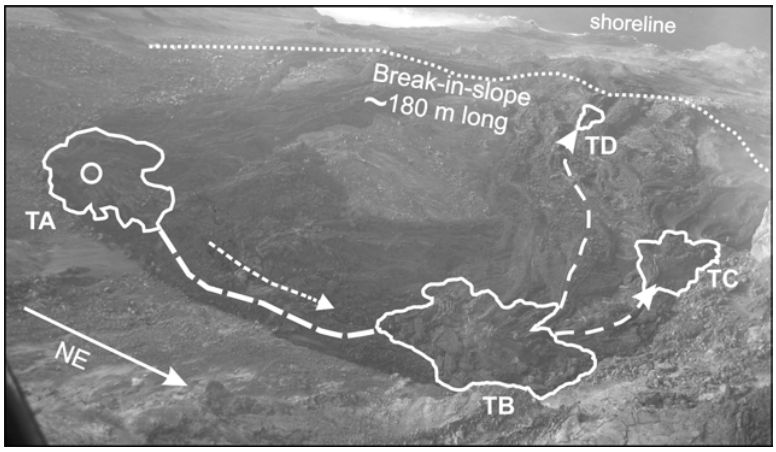

Figure 4

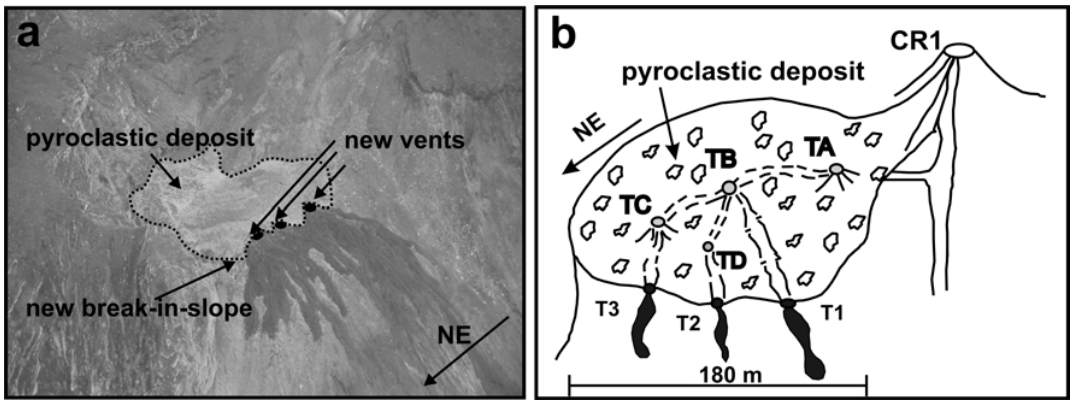
a
pyroclastic deposit
new vents
new break-in-slope
NE
b
CR1
pyroclastic deposit
NE
TB
TA
TC
TD
T3
T2
T1
180 m

Figure 5

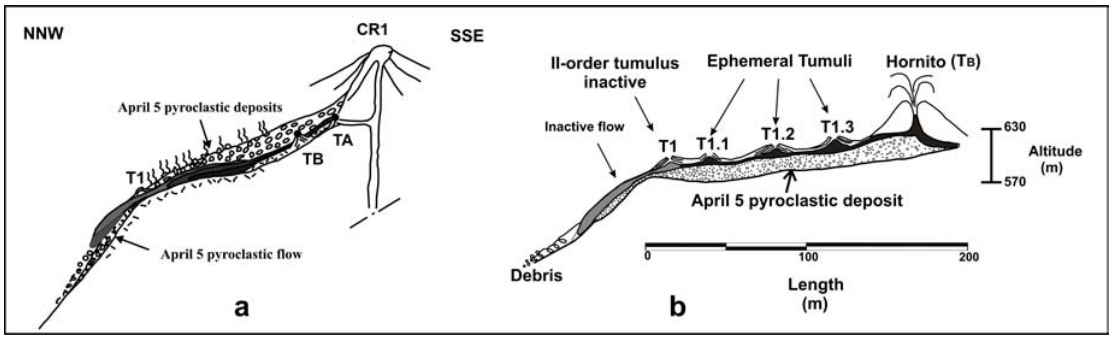
NNW
CR1
SSE
April 5 pyroclastic deposits
TA
TB
T1
April 5 pyroclastic flow
a
II-order tumulus inactive
Ephemeral Tumuli
Hornito (TB)
Inactive flow
T1
T1.1
T1.2
T1.3
630
570
Altitude (m)
April 5 pyroclastic deposit
Debris
0
100
200
Length (m)
b

Figure 6

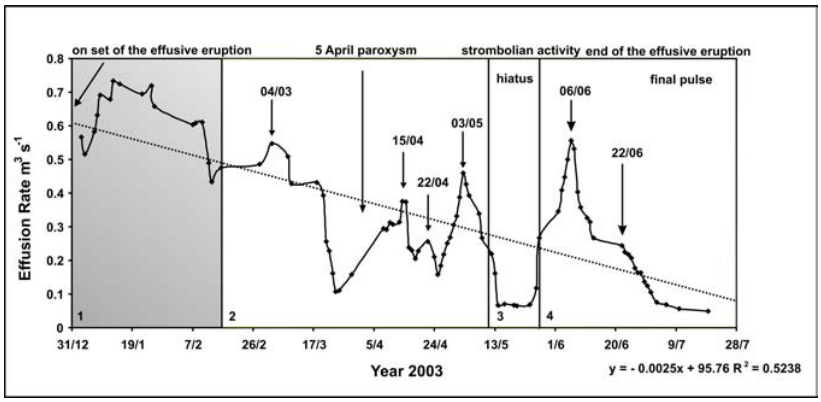
on set of the effusive eruption
5 April paroxysm
strombolian activity
end of the effusive eruption
hiatus
final pulse
04/03
15/04
22/04
03/05
06/06
22/06
Effusion Rate m3 s-1
0.8
0.7
0.6
0.5
0.4
0.3
0.2
0.1
0
1
2
3
4
31/12
19/1
7/2
26/2
17/3
5/4
24/4
13/5
1/6
20/6
9/7
28/7
Year 2003
y = - 0.0025x + 95.76 R2 = 0.5238

Figure 7

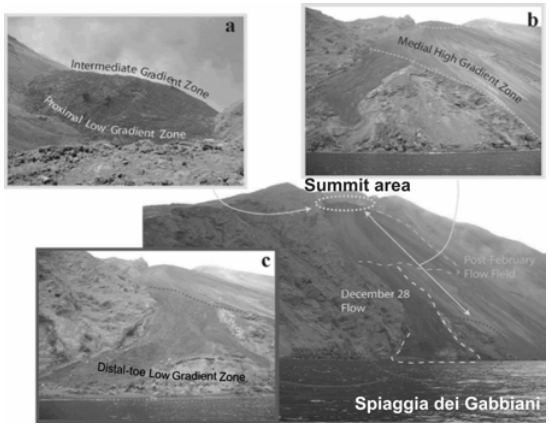
a
Intermediate Gradient Zone
Proximal Low Gradient Zone
b
Medial High Gradient Zone
Summit area
c
Distal-toe Low Gradient Zone
Post February Flow Field
December 28 Flow
Spiaggia dei Gabbiani

Figure 8